*Polymer Composites*

WILEY | spe INSPIRING PLASTICS PROFESSIONALS

RESEARCH ARTICLE OPEN ACCESS

# Development of Flame Retarded Battery Casings Using Glass Fiber-Reinforced Epoxy Resin

Ákos Pomázi[1,2,3] | Zsófia Kovács[1,2] | Beáta Szolnoki[4] | Gábor Szebényi[1,2,5] | Andrea Toldy[1,2]

[1]Department of Polymer Engineering, Faculty of Mechanical Engineering, Budapest University of Technology and Economics, Budapest, Hungary | [2]MTA-BME Lendület Sustainable Polymers Research Group, Budapest University of Technology and Economics, Budapest, Hungary | [3]HUN-REN–BME Research Group for Composite Science and Technology, Budapest, Hungary | [4]Department of Organic Chemistry and Technology, Faculty of Chemical Technology and Biotechnology, Budapest University of Technology and Economics, Budapest, Hungary | [5]Polymeron Ltd, Budapest, Hungary

**Correspondence:** Andrea Toldy (atoldy@edu.bme.hu)

**Received:** 17 June 2026 | **Revised:** 23 July 2026 | **Accepted:** 10 August 2026

**Keywords:** battery casings | electrical resistivity | epoxy composites | flame retardancy

## ABSTRACT

This study investigates the development of glass fiber-reinforced epoxy resin composites with enhanced fire performance for application in electric vehicle battery casings. A low-viscosity epoxy system incorporating phosphorus-, inorganic-, and nitrogen-based (PIN) flame retardants was designed, with particular focus on achieving synergistic effects between ammonium polyphosphate (APP), titanium dioxide ($TiO_2$) and talcum. A multi-stage evaluation strategy was applied, including preliminary screening (TGA, LOI, UL-94, DSC, DMA), followed by detailed characterization of rheological behavior, fire performance under simulated real-fire conditions (cone calorimetry, glow wire flammability index), and mechanical, electrical, and microstructural properties of the resulting composites. The combination of APP and $TiO_2$ exhibited a pronounced synergistic effect, enabling UL-94 V-0 classification in reinforced composites at 4 mm thickness. Cone calorimetry revealed a 53% reduction in peak heat release rate, attributed to enhanced char formation and stabilization of the protective layer. Importantly, the incorporation of solid flame retardants with appropriate morphology did not compromise the glass transition temperature ($T_g > 135°C$) and resulted in only minor reductions in flexural properties (< 10%), while electrical resistivity remained unchanged. The results demonstrate that the appropriate selection and combination of solid flame retardants enables the decoupling of fire performance from thermomechanical degradation, providing a viable pathway for the development of multifunctional composite materials for fire-safe battery enclosure applications.

## 1 | Introduction

Composite parts are increasingly used in electric vehicles due to their excellent mechanical properties and low weight. Weight reduction also has significant environmental benefits, as using composite structures can reduce carbon dioxide emissions and vehicle energy consumption [1]. Currently, aluminium components are mainly used in electric vehicles, while composite structures account for only a small proportion. Using metal components obviously means higher weight and, thus, higher environmental impact. In contrast, composite structures can significantly reduce the overall footprint [2–4]. A major disadvantage of composites compared to metals, however, is their flammability, which is a significant factor in all automotive applications, especially in electric vehicles. Ensuring passenger safety in vehicles, particularly electric ones, is crucial. One way to enhance safety is to incorporate flame-retardant composite materials into battery housings. This can potentially prolong the time available for escape during a battery fire by several minutes, ultimately saving lives. The flame retardancy of polymer composites can be achieved by the flame retardancy of the polymer matrix and/or reinforcing fibers, or by

**Highlights**

- APP–$TiO_2$ synergy enabled UL-94V-0 and GWFI 960/4.0 in epoxy/glass composites
- coherent ceramic–phosphate layer stabilized condensed-phase action
- peak heat release rate decreased by 53% in cone calorimetry
- $T_g$ increased from 139°C to 141°C for TRAC 5%P APP 5% $TiO_2$ composite
- flexural modulus, strength and electrical resistivity were largely unaffected

using flame retardant coatings [5–7]. The flame retardancy of the matrix material often leads to a reduction in mechanical properties and the glass transition temperature, although in the case of inert fibers like glass, rather the polymer matrix is flame retarded. Coatings are applied when the additional mass is acceptable, and the possible heat source leading to a fire can be well located [8–10].

In the context of sustainable development, flame retardants must have minimal impact on health and the environment throughout their entire life cycle, including during recycling and disposal. As a result, there has been a growing emphasis on halogen-free additives, particularly PIN (phosphorus-, inorganic-, and nitrogen-containing) flame retardants [11–13].

One of the major obstacles in achieving flame retardancy is that the fire performance of composite materials is often inversely related to their mechanical properties [14, 15]. This is especially true for many flame retardants, which can significantly reduce the glass transition temperature ($T_g$) of the composites due to their softening effect. Nevertheless, based on the authors' previous experience, certain spherical solid flame retardants do not decrease the $T_g$ and may even increase it [16]. The main idea of the study was to combine PIN flame retardants that do not affect the $T_g$ and have different flame retardant mechanisms and to exploit their synergistic combination in terms of fire performance and mechanical properties.

For this purpose, APP was combined with talc and $TiO_2$. According to the literature, the effect of talc lies mainly in the formation of a ceramified charred residue, showing high dimensional and increased thermal stability and good mechanical strength [17, 18]. Together with glass fibers, it was concluded that the mechanical properties deteriorated to some extent with the combined use of ammonium polyphosphate and talc due to the addition of flame retardants [19]. However, this study did not address the effect of this additive combination on the glass transition temperature, which is a critical parameter for industrial applications such as electric vehicle battery casing. $TiO_2$ together with APP was proved to be beneficial in terms of flame retardancy in some polymer matrices [20, 21]. $TiO_2$ can reduce the oxidation of the char, and can form inorganic $TiP_2O_7$, [22] leading to higher residual weight, while the formation of Ti-O-Ti network enhances the structure of the char so that the flammable decomposition products can be retained; leading to increased LOI values, and decreased heat release values [20].

This study aimed to develop fire-resistant battery casings using glass fiber-reinforced epoxy resin composites. For that, we have defined the following requirements:

- Achieving a UL-94 V-0 self-extinguishing rating,
- Limiting the reduction in mechanical properties to less than 10% compared to the reference composite,
- Attaining a glass transition temperature above 100°C.

## 2 | Materials and Methods

An epoxy system consisting of EPIKOTE Resin TRAC and EPIKURE Curing Agent TRAC (Westlake, Houston, Texas, USA) was used. The main component of the epoxy resin is diglycidyl ether of bisphenol A (DGEBA), while the curing agent is primarily based on triethylenetetramine (TETA). As flame retardants, we used ammonium polyphosphate (APP; trade name: NORD-MIN JLS APP; producer: Nordmann Rassmann, Hamburg, Germany; P content: 31%–32%; average particle size: 15 μm), rutile-type titanium dioxide ($TiO_2$; particle size distribution Dv(10) = 0.25 μm, Dv(50) = 0.59 μm, Dv(90) = 1.30 μm, producer: Cinkarna, Celje, Slovenia), and talcum (type: IMI Fabi Talc HTPultra5c, average particle size: 0.5 μm producer: IMI Fabi, Milan, Italy). The flame retardants (FR) were mixed into the epoxy component, then the hardener was added, and the mixture was poured into a silicone mold and cured for 15 min at 140°C. The normalized mass fractions of the applied components are summarized in Table 1. According to DSC tests, the curing was complete, and the $T_g$ of the TRAC reference system was 141.6°C.

For initial flammability screening, 2 mm thick composite laminates were produced using SAERTEX 30003318 7,000,174-08008811-635 glass fiber reinforcement (397 g/$m^2$ areal weight). Individual reinforcement layers were impregnated separately with resin by hand lamination directly in the press mold. The laminates were consolidated in a temperature-controlled platen press (T30, Metal Fluid Engineering s.r.l., Verdello Zingonia, Italy) under a hydraulic pressure of 180 bar (corresponding to 25 bar applied to the laminate) and cured at 140°C for 10 min. The resulting 2 mm thick laminates were produced in a $[0]_6$ lay-up, yielding a fiber content of 60 ± 1 mass%.

For up-scaled composite production, 4 mm thick laminates were manufactured by wet compression molding using a twill weave glass fiber fabric (GW 123–580 K2, R&G Faserverbundwerkstoffe GmbH, Waldenbuch, Germany; 580 g/$m^2$ areal weight, silane sizing), with the main manufacturing steps summarized in Figure 1. To minimize void formation, an anti-bubble agent (HP-BEL51, HP-Textiles, Schapen, Germany) was added at 0.8 mass% relative to the matrix mass. Prior to processing, the fabric was dried for 4 h at 80°C to remove absorbed moisture. Four reinforcement plies were first placed into the mold and impregnated with approximately half of the resin formulation, followed by stacking of four additional plies and application of the remaining resin.

This two-step impregnation approach ensured complete fiber wetting, as simultaneous impregnation of all eight layers resulted in insufficient resin penetration with the T30 platen press. The mold was inserted into the platen press and heated gradually from 25°C to 100°C while maintaining a hydraulic pressure of 180 bar (25 bar on the laminate). Consolidation was carried out for 8 min, producing 4 mm thick laminates with a $[0]_8$ lay-up. This manufacturing strategy was selected to model industrial composite production routes used for structural battery casing components.

We determined the enthalpy of curing and $T_g$ by differential scanning calorimetry (DSC) with TA Instruments Q2000 (New Castle, USA). We studied the thermal degradation of epoxy resins using a TA Instruments Q5000 TGA device (New Castle, USA) over the temperature range of 25°C–800°C at a heating rate of 10°C $min^{-1}$ in $N_2$ atmosphere. We characterized the fire performance using the limiting oxygen index (LOI, according to ASTM D2863), UL-94 tests conducted in accordance with ASTM D3801 and ASTM D635, mass loss type cone calorimetry according to ISO 13927 at 50 $kW/m^2$ heat flux, with a device from FTT Inc. (East Grinstead, UK), pyrolysis combustion flow calorimetry (PCFC) with FTT Inc. (East Grinstead, UK) equipment and glow wire flammability index (GWFI) testing using a Glow Wire Tester T4-08 (Testing d. o. o., Slovenia) in accordance with IEC 60695. Viscosity was determined by parallel plate rheometry using an AR2000 device from TA Instruments (New Castle, DE, USA) in the 25°C–80°C range, with a 5°C/min temperature ramp and 25 1/s shear rate. We investigated the dynamic mechanical properties and $T_g$ of the composite samples using a TA Instruments Q800 device (New Castle, USA) in a three-point bending arrangement. The samples were tested in a temperature range of 25°C–200°C with a heating rate of 3°C $min^{-1}$. The three-point bending tests were conducted according to EN ISO 14125 using a Zwick Z005 computer-controlled tensile tester (Zwick GmbH, Ulm, Germany) equipped with a 5 kN capacity load cell. The support span was 40 mm, and the test speed was 2 mm/min. The flatwise Charpy impact tests were carried out according to EN ISO 179-1 with a CEAST Resil Impactor Junior pendulum equipped with a 15 J impact energy hammer.

**TABLE 1** | Normalized mass fractions applied in reference and flame retarded epoxy systems.

| Sample | Epoxy | Curing agent | APP | $TiO_2$ | Talcum |
|---|---|---|---|---|---|
| TRAC REF | 0.8621 | 0.1379 | 0 | 0 | 0 |
| TRAC 3%P APP | 0.7800 | 0.1248 | 0.0952 | 0 | 0 |
| TRAC 5%P APP | 0.7253 | 0.1160 | 0.1587 | 0 | 0 |
| TRAC 3%P APP 5% $TiO_2$ | 0.7369 | 0.1179 | 0.0952 | 0.05 | 0 |
| TRAC 3%P APP 5% talcum | 0.7369 | 0.1179 | 0.0952 | 0 | 0.05 |
| TRAC 5%P APP 5% $TiO_2$ | 0.6822 | 0.1091 | 0.1587 | 0.05 | 0 |

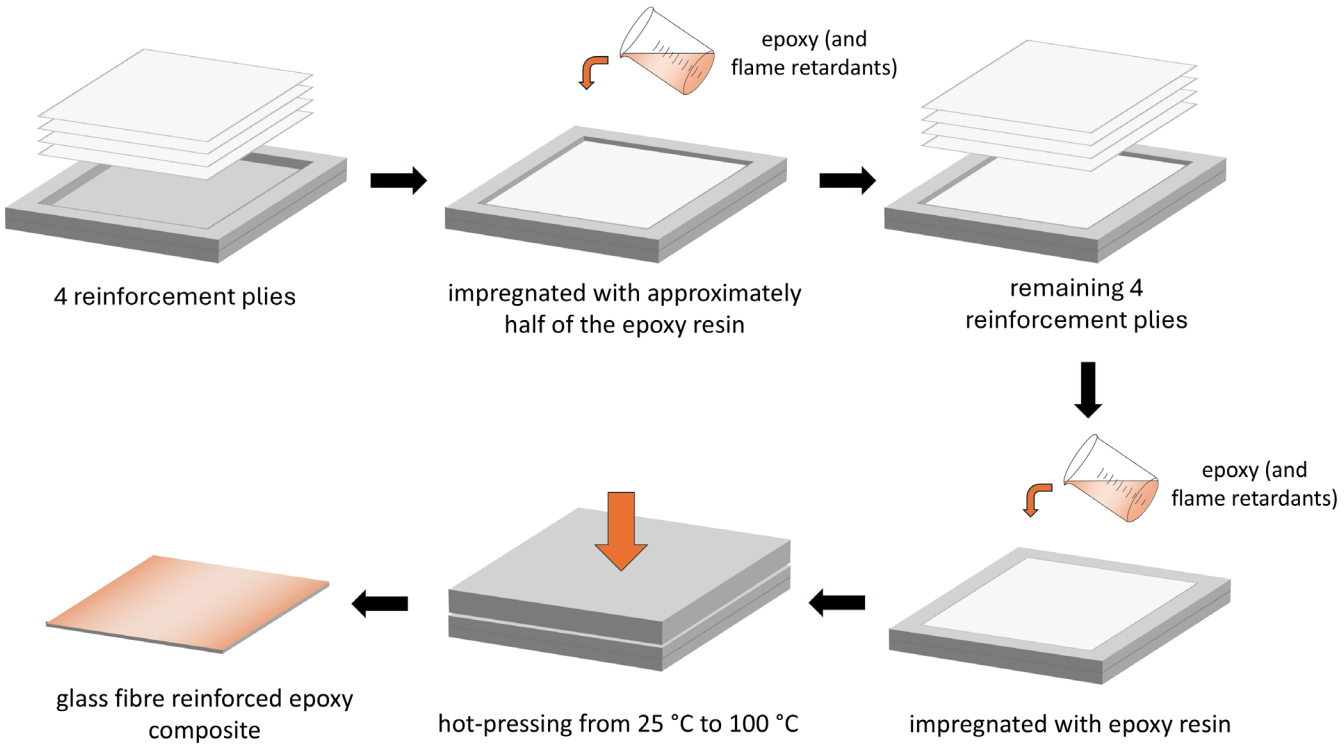


**FIGURE 1** | Schematic overview of the wet compression molding process used for manufacturing the up-scaled glass fiber reinforced epoxy composite laminates.

**TABLE 2** | Thermal and fire performance of the epoxy systems.

| Sample | LOI (V/V%) | UL-94 (mm/min) | PCFC THR (kJ/g) | $T_{-5\%}$ (°C) | $dTG_{max}$ (%/°C) | Residue (%) |
|---|---|---|---|---|---|---|
| TRAC REF | 22 | HB (22.97) | 27.46 | 335.5 | 1.485 | 6.8 |
| TRAC 3%P APP | 28 | HB (vertical 1) | 22.96 | 306.4 | 1.386 | 18.1 |
| TRAC 5%P APP | 32 | V-1 | 22.74 | 303.8 | 1.294 | 17.9 |
| TRAC 3%P APP 5% $TiO_2$ | 32 | V-0 | 23.71 | 310.3 | 1.430 | 21.6 |
| TRAC 3%P APP 5% talcum | 32 | V-0 | 24.20 | 307.0 | 1.315 | 19.3 |
| TRAC 5%P APP 5% $TiO_2$ | 35 | V-0 | 18.50 | 307.9 | 1.215 | 26.2 |

*Note:* PCFC THR, pyrolysis combustion flow calorimetry total heat release; $T_{-5\%}$, temperature at 5% mass loss; $dTG_{max}$, maximum mass loss rate; residue, TGA residue at 800°C.

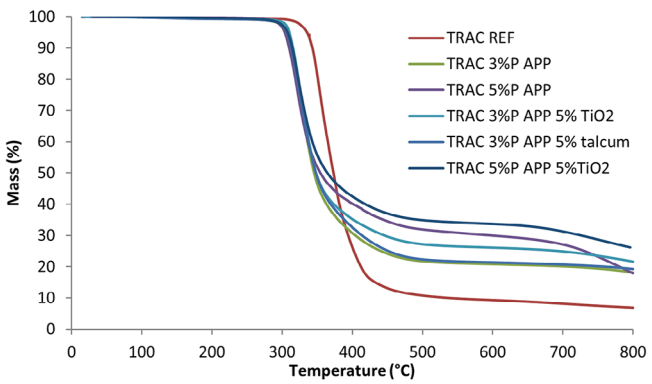


**FIGURE 2** | Thermal stability of reference and flame retarded epoxy resin matrix samples.

The impact angle was 150°, the impact velocity was 3.7 m/s, and the impact energy was 15 J. The porosity was determined in accordance with ASTM D2734, taking into account the fiber and additive content of the composite. The density measurement required for determining porosity was performed in accordance with ASTM D792. The electrical resistivity of the samples was measured in a four-point setup using an Agilent digital multimeter for data acquisition. The 80 × 10 mm samples were used for the measurement. The resistance values were evaluated after 2 min to avoid transient effects. Scanning electron microscopy coupled with energy-dispersive x-ray spectrometry (SEM–EDS) was performed using a JEOL JSM 6380LA instrument (JEOL Ltd., Tokyo, Japan). Cross-sections of the composite specimens were examined after gold sputter coating with a JEOL JPC1200 device to prevent surface charge accumulation.

## 3 | Results

First, a preliminary screening was performed using TGA, LOI, UL-94, PCFC, DSC and DMA analyses. Based on these results, the most promising formulations were selected for further investigation, including rheological characterization of the matrix resin, fire performance under simulated real-fire conditions (mass loss type cone calorimetry, glow wire flammability index), flexural and impact properties, as well as the electrical resistivity, porosity of the composites, and the filtration behavior of the solid additives.

### 3.1 | Thermal Degradation and Fire Performance

The initial thermal and fire retardancy screening results of the reference and flame retarded epoxy resin matrix samples are summarized in Table 2. The mass-temperature curves of the reference and flame-retarded epoxy resin samples obtained from the TGA measurements are presented in Figure 2.

In matrix samples, APP alone was insufficient to achieve V-0 classification; however, combining 3%P from APP (equivalent to 9% APP) with 5 mass% $TiO_2$ or talcum already resulted in V-0 performance. The reduced THR values together with increased residue formation indicate effective condensed-phase flame-retardant action and intumescent char development. The shift toward lower $T_{-5\%}$ reflects early phosphorus activation, enabling protective char formation before rapid polymer volatilization occurs. The reduction in maximum mass loss rate confirms suppressed degradation intensity and reduced combustible gas evolution. Among the investigated systems, the APP/$TiO_2$ formulations show the most pronounced increase in residue, indicating a strong synergistic effect that stabilizes the char structure.

Despite the presence of 60 mass% inert glass fibers, achieving flame retardancy in composite laminates proved more demanding (Table 3, Figure 3). The synergistic interaction between APP and $TiO_2$ was more effective than with talcum; therefore, in addition to the reference formulation, composites containing 3%P from APP and 5 mass% $TiO_2$, and 5%P from APP and 5 mass% $TiO_2$, respectively, were prepared at a more application-relevant thickness of 4 mm. Among these, the formulation containing 5%P from APP and 5 mass% $TiO_2$ achieved the V-0 classification at 4 mm thickness, thereby fulfilling the predefined performance requirement.

The more moderate improvement observed in composite systems reflects the influence of the glass fibers on heat transfer and flame propagation, which can limit the effectiveness of matrix-based flame-retardant mechanisms. Achieving V-0 at increased

thickness demonstrates that sufficient phosphorus loading combined with $TiO_2$ effectively promotes condensed-phase flame retardancy even in fiber-reinforced laminates. Overall, these results underline the importance of optimizing flame-retardant formulations at the composite level, as matrix performance alone does not directly predict laminate fire behavior.

### 3.2 | Glass Transition Temperature

The glass transition temperature of the epoxy resins and their composites is listed in Table 4.

The glass transition temperature of flame retarded matrix and composite specimens remained in the same region as the reference.

**TABLE 3** | LOI and UL-94 test results of glass fiber reinforced composite laminates.

| Composite sample | LOI (V/V%) | UL-94 |
|---|---|---|
| TRAC REF 2 mm | 28 | HB (vertical 1) |
| TRAC 3%P APP 2 mm | 27 | HB (vertical 1) |
| TRAC 5%P APP 2 mm | 26 | HB (vertical 2) |
| TRAC 3%P APP 5% $TiO_2$ 2 mm | 29 | HB (vertical 1) |
| TRAC 3%P APP 5% talcum 2 mm | 27 | HB (vertical 1) |
| TRAC REF 4 mm | 29 | HB (vertical 1) |
| TRAC 3%P APP 5% $TiO_2$ 4 mm | 29 | V-1 |
| TRAC 5%P APP 5% $TiO_2$ 4 mm | 29 | V-0 |

The minor decrease in matrix $T_g$ observed suggests a limited plasticising or network-modifying effect of the flame-retardant additive, although the reduction remains within experimental uncertainty. The nearly unchanged $T_g$ values of the composites indicate that the incorporation of flame retardants did not significantly affect the curing efficiency or crosslink density of the epoxy network. The slightly broader tanδ peaks (Figure 4) observed for certain formulations imply a marginal increase in network heterogeneity, which can be attributed to the presence and dispersion state of solid additives within the matrix. The slight decrease in $T_g$ observed for the TRAC 3%P APP 5% $TiO_2$ composite is likely associated with local network heterogeneity arising from the incorporation and dispersion of the solid additives. In contrast, the higher APP loading in the TRAC 5%P APP 5% $TiO_2$ formulation appears to compensate for this effect through enhanced restriction of polymer chain mobility, resulting in a $T_g$ that slightly exceeds that of the reference composite. All compositions passed our initial criteria of reaching a glass transition temperature above 100°C. Notably, the TRAC 5%P APP 5% $TiO_2$ composite sample exhibited the highest $T_g$ among all formulations, slightly exceeding even the reference value, while also demonstrating the best flame retardancy with a V-0 rating in the UL-94 test.

### 3.3 | Dynamic Mechanical Properties

The dynamic mechanical behavior of the reference and flame retarded composites was investigated using DMA. We determined the storage modulus at 25°C (room temperature) and at a higher temperature (75°C) to determine if any decrease appears. The results are summarized in Table 5.

The storage modulus of composite samples at 25°C and 75°C remained in the same range as the reference. In cases where the storage modulus decreased slightly, the decrease was less than 10%. This limited variation indicates that the incorporation of flame-retardant additives does not significantly impair

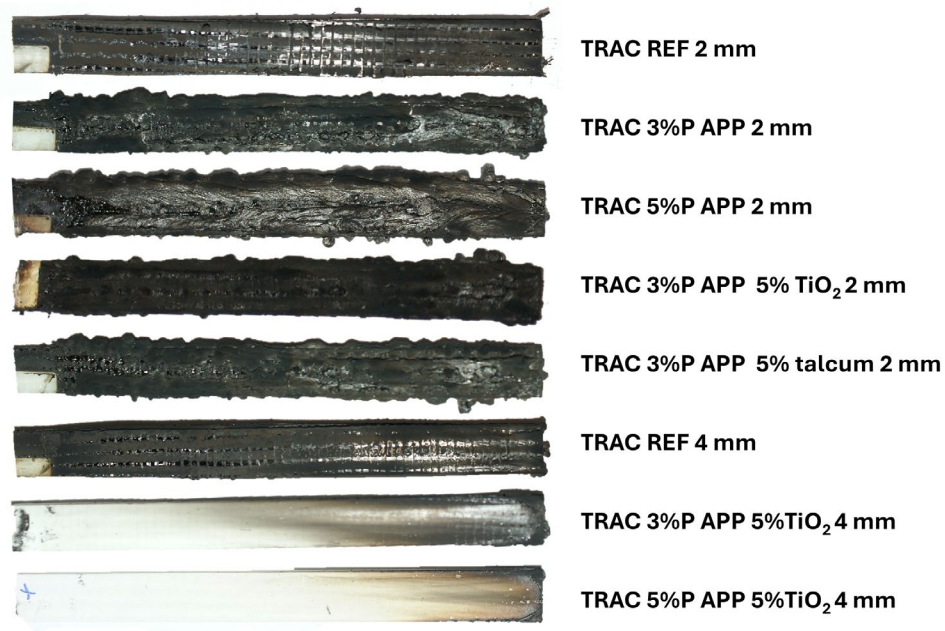


**FIGURE 3** | UL-94 composite specimens after the vertical test.

the load-bearing capability of the fiber-reinforced structure. Minor modulus reductions observed for some APP-containing formulations are attributed to local heterogeneities and subtle modifications of fiber–matrix interfacial interactions introduced by solid additives. With increasing APP content alone or upon talcum addition, the initially observed modulus-reducing effects are compensated and transition into a reinforcing filler behavior, resulting in a slight modulus increase for the TRAC 5%P APP and TRAC 3%P APP 5% talcum formulations.

In contrast, the APP–$TiO_2$ system exhibits a different trend, indicating that $TiO_2$ changes the role of APP from a passive rigid filler to a chemically interacting flame-retardant phase. The resulting interactions likely modify the fiber–matrix interphase, explaining the moderate stiffness reduction despite improved fire performance. The TRAC 5%P APP 5% $TiO_2$ composite, therefore, represents a balanced response: although the storage modulus decreases slightly (−7.6% at 25°C and −9.9% at 75°C), the values remain within the predefined acceptable limit (< 10%). The comparable modulus retention at 75°C demonstrates that thermomechanical stability is preserved below the glass transition region, confirming that flame-retardant incorporation does not compromise service-temperature performance. Overall, the DMA results demonstrate that enhanced flame retardancy can be achieved without sacrificing structural integrity, confirming the targeted balance between mechanical performance and fire safety.

Based on the preliminary screening results from TGA, LOI, UL-94, PCFC, DSC, and DMA analyses, further investigations were conducted with the TRAC reference formulation and the optimized flame-retarded system TRAC 5%P APP 5% $TiO_2$, which achieved the required fire-performance level while maintaining acceptable thermomechanical properties. The previously investigated TRAC 3%P APP 5% $TiO_2$ formulation served as an intermediate composition; however, the higher APP loading proved necessary to reach UL-94 V-0 classification and was therefore selected for the subsequent up-scaled fire and mechanical evaluations.

**TABLE 4** | $T_g$ of the matrix samples determined from DSC and the $T_g$ of the composites determined from DMA.

| Sample | Matrix $T_g$ from DSC (°C) | Δ (%) | Composite $T_g$ from DMA (°C) | Δ (%) |
|---|---|---|---|---|
| TRAC REF | 141.6 | | 138.7 | |
| TRAC 3%P APP | 137 | −3.2 | 138.7 | 0 |
| TRAC 5%P APP | 137.8 | −2.7 | 138.8 | 0.1 |
| TRAC 3%P APP 5% $TiO_2$ | 141 | −0.4 | 135.1 | −2.6 |
| TRAC 3%P APP 5% talcum | 138.8 | −2.0 | 139.6 | 0.6 |
| TRAC 5%P APP 5% $TiO_2$ | 141.1 | −0.3 | 141.2 | 1.8 |

## 3.4 | Rheological Testing

The incorporation of solid particles increases the viscosity of the epoxy resin, whereas increasing the temperature reduces viscosity until the onset of the crosslinking reaction. Thus, an optimal viscosity range should be determined, with manufacturability as the primary focus. We investigated the temperature dependence of viscosity for the three chosen compositions. The results are shown in Figure 5 and Table 6.

We aimed to optimize the viscosity for the hot-pressing method, which requires a viscosity below 1000 mPa·s; however, for rapid processing and improved fiber wetting, viscosities below 500 mPa·s are preferred.

The rheology results showed that both flame retarded compositions passed these criteria. The TRAC 5%P APP 5% $TiO_2$ flame retarded resin reached a viscosity of 1000 mPa·s at approximately 39°C and 500 mPa·s at around 45°C. As TRAC must be preheated to 60°C–80°C before processing according to the manufacturer,

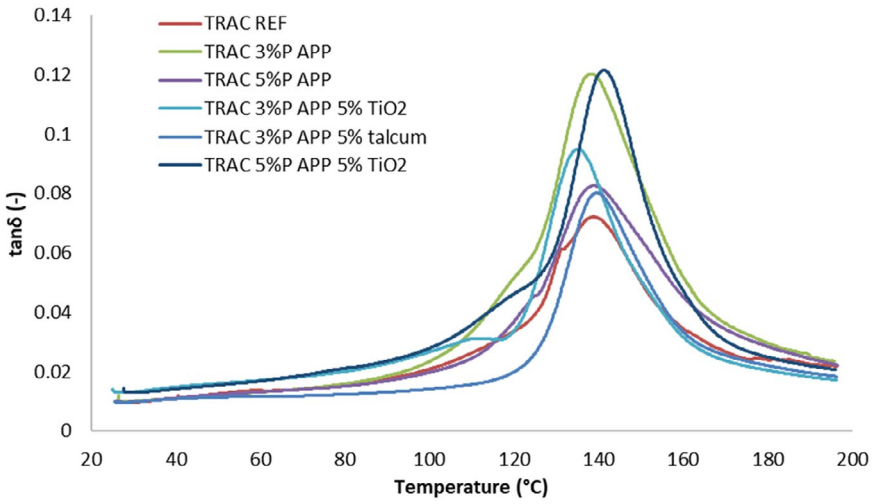


**FIGURE 4** | Tanδ results of the reference and flame retarded epoxy resin composite samples.

this requirement is satisfied. These results demonstrate that incorporating APP and $TiO_2$ only moderately increases viscosity, indicating that the selected filler loading remains compatible with industrial composite processing routes. The similar viscosity–temperature profiles of the formulations suggest that particle addition does not significantly alter the resin flow behavior before curing onset. At the recommended processing temperatures (60°C–80°C), all systems exhibit sufficiently low viscosity to ensure effective fiber impregnation and minimize voids during hot pressing. Since the difference between the two formulations with different APP concentrations is within the range of experimental variation and the higher APP content also provides suitable processability while being necessary to achieve the UL-94 V-0 classification, the following investigations focus on the TRAC 5%P APP 5% $TiO_2$ system.

**TABLE 5** | Storage moduli of the composite samples.

| Composite | Storage modulus at 25°C (MPa) | Δ (%) | Storage modulus at 75°C (MPa) | Δ (%) |
|---|---|---|---|---|
| TRAC REF | 28,486 | | 27,406 | |
| TRAC 3%P APP | 26,841 | −5.8 | 25,283 | −7.7 |
| TRAC 5%P APP | 29,058 | 2.0 | 27,627 | 0.8 |
| TRAC 3%P APP 5% $TiO_2$ | 26,763 | −6.0 | 24,778 | −9.6 |
| TRAC 3%P APP 5% talcum | 29,813 | 4.7 | 29,434 | 7.4 |
| TRAC 5%P APP 5% $TiO_2$ | 26,328 | −7.6 | 24,701 | −9.9 |

## 3.5 | Mass Loss Type Cone Calorimetry

Based on the preliminary screening results, a formulation containing 5%P APP and 5% $TiO_2$ was required to achieve UL-94 V-0 classification; therefore, up-scaled fire performance and mechanical testing were performed on these samples. Figure 6 shows the heat release date curves of the TRAC reference and TRAC 5%P APP 5% $TiO_2$ matrices and their composites, while Table 7 summarizes the numerical mass loss type cone calorimetry results. Optical microscopy images of the mass loss type cone calorimetry composite residues are presented in Figure 7.

The peak heat release rate decreased significantly simply with the inclusion of the fibrous media. The addition of the 5%P APP 5% $TiO_2$ flame retardant additive system further decreased the pHRR from 343 kW/m$^2$ to 160 kW/m$^2$, resulting in a significant 53% reduction. The pronounced pHRR reduction demonstrates the effective control of fire growth intensity, a critical parameter for delaying flashover in real fire scenarios. In the matrix

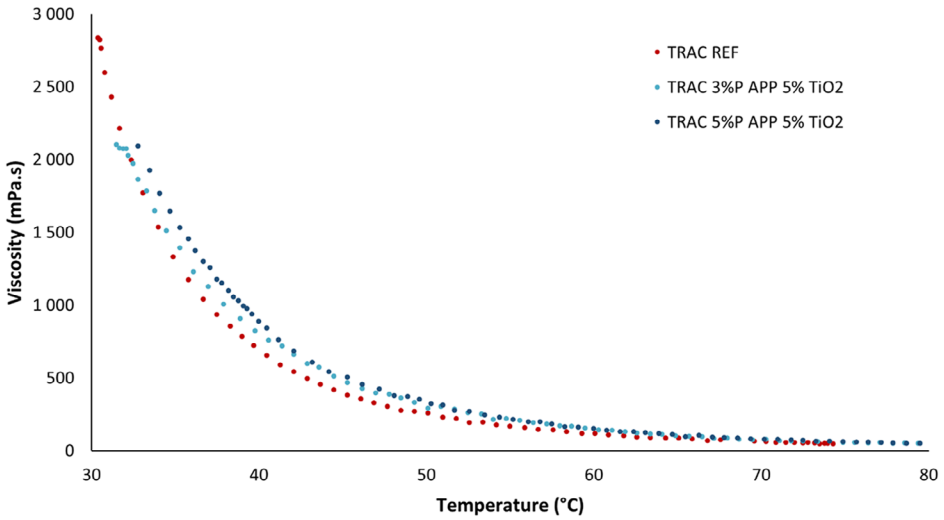


**FIGURE 5** | The viscosity of the chosen epoxy matrices.

**TABLE 6** | Rheology test results of epoxy compositions.

| TRAC REF | | TRAC 3%P APP 5% $TiO_2$ | | TRAC 5%P APP 5% $TiO_2$ | |
|---|---|---|---|---|---|
| Temperature (°C) | Viscosity (mPa.s) | Temperature (°C) | Viscosity (mPa.s) | Temperature (°C) | Viscosity (mPa.s) |
| 36.7 | 1040 | 37.9 | 1007 | 38.8 | 1032 |
| 42.9 | 497 | 44.5 | 512 | 45.3 | 504 |
| 60.1 | 116.8 | 60.3 | 142 | 60.0 | 152 |

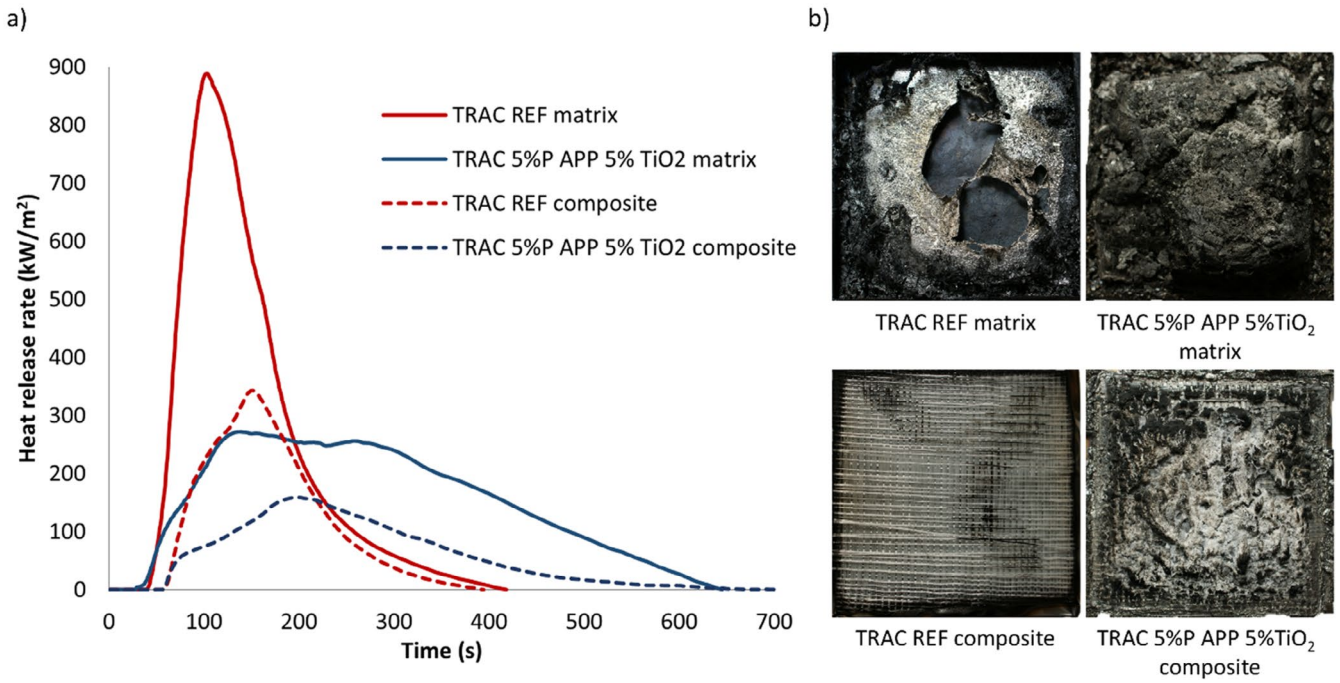


**FIGURE 6** | Heat release rate (a) and residue (b) of the TRAC reference and TRAC 5%P APP 5% $TiO_2$ matrices and their composites.

**TABLE 7** | Mass loss type cone calorimetry results of the TRAC reference and TRAC 5%P APP 5% $TiO_2$ matrices and their composites.

| Sample | TTI (s) | pHRR (kW/m²) | $t_{pHRR}$ (s) | THR (MJ/m²) | Residue (%) |
|---|---|---|---|---|---|
| TRAC REF matrix | 37 | 888 | 103 | 99.01 | 1 |
| TRAC 5%P APP 5% $TiO_2$ matrix | 25 | 272 | 139 | 97.56 | 24 |
| TRAC REF composite | 58 | 343 | 151 | 44.87 | 60 |
| TRAC 5%P APP 5% $TiO_2$ composite | 56 | 160 | 198 | 39.12 | 64 |

*Note:* TTI: time to ignition, pHRR: peak heat release rate, $t_{pHRR}$: time to pHRR, THR: total heat release; Average standard deviation of the measured mass loss calorimeter values: TTI: ±3; pHRR: ±30; $t_{pHRR}$: ±5; THR: ±3 residue: ±2.

systems, the APP/$TiO_2$ combination promotes early char formation, as reflected in increased residue yield and a delayed pHRR. The shift of the pHRR to longer times indicates the formation of a thermally stable protective layer that slows heat and mass transfer between the flame and the underlying material. In composite laminates, the already reduced heat release due to the non-combustible glass fiber structure is further improved by the flame-retardant matrix, confirming that condensed-phase protection remains effective in the reinforced system. The reference composite exhibited almost complete degradation of the epoxy matrix, leaving the glass fabric clearly exposed with only minor carbonaceous residue. In contrast, the TRAC 5%P APP 5% $TiO_2$ composite formed a continuous expanded char layer with a porous, foam-like morphology covering the reinforcement (Figure 7). Bright regions observed within the residue are consistent with the presence of inorganic combustion products, potentially associated with the titanium-containing additive.

Overall, the combined effect of fiber reinforcement and the flame-retardant action of APP/$TiO_2$ results in a substantially improved fire performance without compromising composite integrity. This behavior suggests that $TiO_2$ interacts with the APP-derived polyphosphate phase, promoting the formation of a mechanically stable ceramic-reinforced char layer that suppresses surface degradation and maintains effective thermal shielding throughout combustion.

### 3.6 | Glow Wire Flammability Index (GWFI)

The GWFI test is widely used in the electronics, electrical, and energy industries, particularly for evaluating the fire resistance of plastic components in electrical enclosures, connectors, circuit breakers, and insulating materials. While these are the most common industrial sectors, the test is also relevant in the automotive industry, especially for electric vehicle parts such as battery casings. In this test, a heated, glowing wire touches the sample for 30 s. After 30 s of contact, the wire is removed from the sample. The standard organizes the samples into different categories based on the material's behavior. In the GWFI rate,


TRAC REF composite 100x


TRAC REF composite 200x

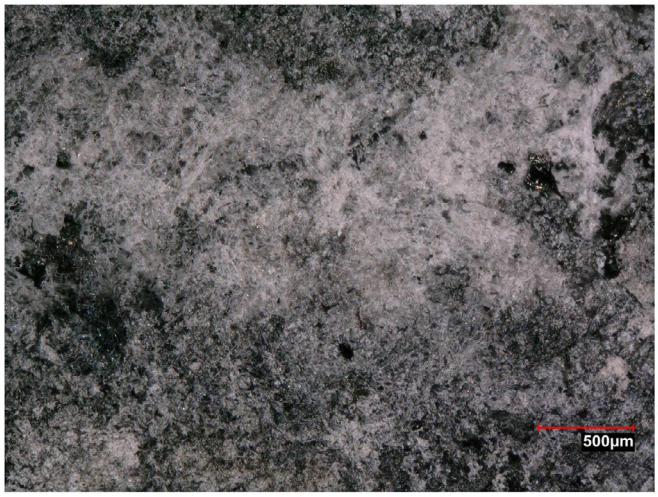


TRAC 5%P APP 5% $TiO_2$ composite 100x

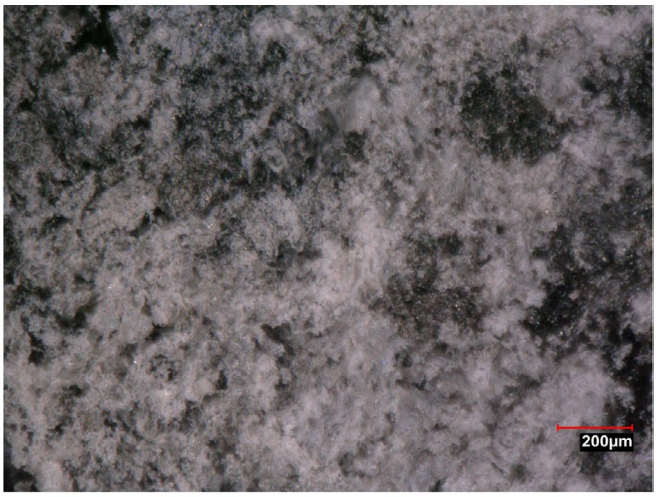


TRAC 5%P APP 5% $TiO_2$ composite 200x

**FIGURE 7** | Optical microscopy images of the TRAC reference and TRAC 5%P APP 5% $TiO_2$ composite residues.

**TABLE 8** | GWFI results of the reference and flame retarded matrices and composites.

| GWFI | | | | |
|---|---|---|---|---|
| **Temperature** | **30 s (contact)** | **After 30 s of contact** | **Note** | **GWFI rate** |
| TRAC REF matrix | | | | |
| 750°C | 10 cm flame | Burnt > 30 s after removing the glow wire | Sample burnt through | |
| 650°C | No burning | No burning | Sample was punctured | 650/4.0 |
| TRAC 5%P APP 5% $TiO_2$ matrix | | | | |
| 960°C | Burnt with a 4 cm flame | Burnt for 5 s after removing the glow wire | Sample burnt through | 960/4.0 |
| TRAC REF composite | | | | |
| 960°C | Burnt with a 1–1.5 cm flame | Burnt 3 s after removing the glow wire | Sooty flame, sample burnt not through | 960/4.0 |
| TRAC 5%P APP 5% $TiO_2$ composite | | | | |
| 960°C | Burnt with a 1–1.5 cm flame | Extinguished immediately after contact | White smoke, sample burnt not through | 960/4.0 |

the first number means the temperature in "°C", while the second number is the thickness of the sample in mm. The samples can be tested at different wire temperatures, where 960°C is the highest. Table 8 shows the GWFI results for the TRAC reference, the TRAC 5%P APP 5% $TiO_2$ matrix, and their composites.

Both the TRAC 5%P APP 5% $TiO_2$ matrix and composite samples reached the highest rating of 960/4.0. The immediate self-extinguishing behavior observed for the flame-retarded composite after glow-wire removal indicates efficient suppression of sustained flaming under severe local thermal loading. Compared to the reference matrix, the reduced afterflame time demonstrates the effectiveness of the APP/$TiO_2$ system in limiting flame propagation once the external ignition source is removed. The formation of white smoke instead of a sooty flame suggests enhanced condensed-phase action and more complete stabilization of degradation products within the protective char layer. Achieving the maximum GWFI classification confirms that the developed formulation fulfills stringent requirements for electrical and battery-related applications, where resistance against ignition by overheated metallic components is critical. The consistent performance of both matrix and composite specimens further indicates that the flame-retardant mechanism remains effective after fiber reinforcement and composite processing.

### 3.7 | Porosity

Although the epoxy resin manufacturer provided technical guidelines for processing, it was necessary to optimize the

**TABLE 9** | Porosity of the reference and flame retarded composites.

| | | TRAC REF composite preheated press, 140°C, 4 min | TRAC REF composite press heated from 25°C to 80°C, 15 min | TRAC REF composite press heated from 25°C to 100°C, 8 min |
|---|---|---|---|---|
| 1 | Porosity V/V% | 10.48 | 6.00 | 5.83 |
| 2 | | 10.16 | 6.41 | 6.45 |
| 3 | | 6.39 | 6.78 | 6.88 |
| Average | | 9.01 | 6.40 | 6.39 |
| Standard deviation | | 2.28 | 0.39 | 0.53 |
| Relative standard deviation | % | 25.28 | 6.05 | 8.28 |

| | | TRAC REF composite press heated from 25°C to 100°C, 8 min with anti-bubble | TRAC REF composite press heated from 25°C to 100°C, 8 min with dried fabric | TRAC REF composite press heated from 25°C to 100°C, 8 min with anti-bubble and dried fabric |
|---|---|---|---|---|
| 1 | Porosity V/V% | 5.96 | 4.43 | 3.95 |
| 2 | | 5.33 | 7.57 | 3.81 |
| 3 | | 3.76 | 5.19 | 2.70 |
| Average | | 5.02 | 5.73 | 3.48 |
| Standard deviation | | 1.13 | 1.63 | 0.69 |
| Relative standard deviation | % | 22.51 | 28.54 | 19.69 |

| | | TRAC 5%P APP 5% $TiO_2$ preheated press, 140°C, 4 min | TRAC 5%P APP 5% $TiO_2$ press heated from 25°C to 80°C, 15 min | TRAC 5%P APP 5% $TiO_2$ press heated from 25°C to 100°C, 8 min with anti-bubble and dried fabric |
|---|---|---|---|---|
| 1 | Porosity V/V% | 13.27 | 7.45 | 5.65 |
| 2 | | 12.56 | 6.74 | 5.71 |
| 3 | | 11.28 | 6.61 | 5.90 |
| Average | | 12.37 | 6.94 | 5.75 |
| Standard deviation | | 1.01 | 0.45 | 0.13 |
| Relative standard deviation | % | 8.16 | 3.64 | 2.28 |

manufacturing procedure of the flame-retarded composites to minimize porosity, as increased porosity can adversely affect mechanical performance under both static and dynamic loading conditions. The porosity test results are listed in Table 9.

We compared the porosity of the composites prepared with the following process parameters:

1. preheated press to 140°C, pressing time 4 min,
2. gradually heated press from 25°C to 80°C, pressing time 15 min,
3. gradually heated press from 25°C to 100°C, pressing time 8 min,
4. gradually heated press from 25°C to 100°C, pressing time 8 min, application of 0.8% anti-bubble agent,
5. gradually heated press from 25°C to 100°C, pressing time 8 min, fabric dried for 4 h at 80°C,
6. gradually heated press from 25°C to 100°C, pressing time 8 min, application of 0.8% anti-bubble agent, and fabric dried for 4 h at 80°C.

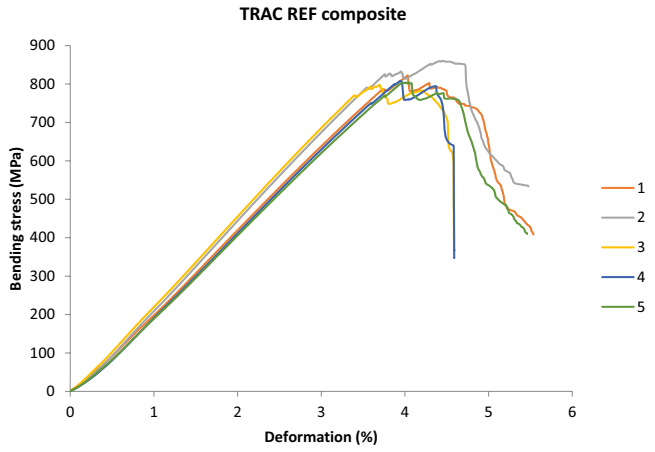


(a) Stress-deformation curves of TRAC REF composites

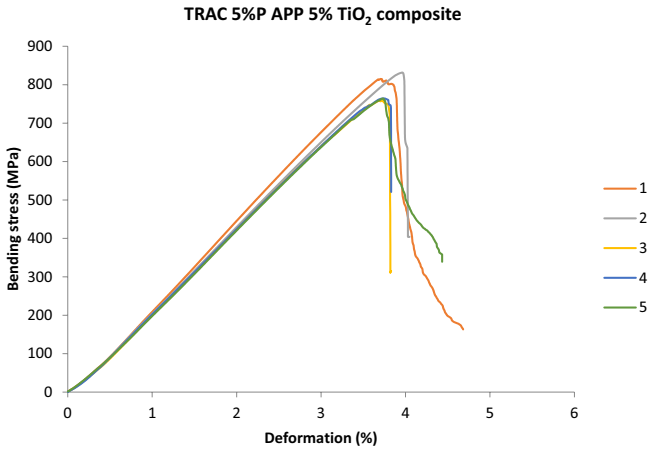


(b) Stress-deformation curves of flame retarded TRAC 5%P APP 5% $TiO_2$ composites

**FIGURE 8** | Stress-deformation curves of the reference (a) and flame-retarded composites (b). (a) Stress-deformation curves of TRAC REF composites, (b) Stress-deformation curves of flame retarded TRAC 5%P APP 5% $TiO_2$ composites.

Both in the TRAC reference and flame retarded composites, the gradual heating to 100°C and the combination of fabric drying and anti-bubble agent lead to the lowest porosity values. With all parameters, the flame retarded composites had a 2%–3% higher porosity. The results clearly demonstrate that rapid heating with a preheated press promotes volatile entrapment and insufficient air evacuation, resulting in significantly higher porosity. Gradual temperature increase allows progressive viscosity reduction and improved resin flow, facilitating gas release before gelation and thereby reducing void formation. Drying of the reinforcement fabric proved particularly effective, indicating that absorbed moisture represents a major source of pore formation during composite consolidation. The additional improvement obtained by the anti-bubble agent confirms that interfacial surface tension effects and bubble stabilization play an important role during the processing of particle-filled flame-retarded systems. The slightly higher porosity observed in flame-retarded composites can be attributed to the presence of solid additives, which locally hinder resin flow and create additional nucleation sites for gas entrapment. Nevertheless, the optimized processing route ensures reproducible laminate quality with low scatter, as reflected by the reduced standard deviation and relative standard deviation values. These findings underline the importance of processing optimization when transferring flame-retardant formulations from neat resins to fiber-reinforced composite manufacturing.

All subsequent mechanical tests were carried out on 4 mm-thick samples produced using optimized process number 6.

### 3.8 | Flexural Modulus of Elasticity and Bending Strength

With the reduction of the porosity in the composite structure, we aimed to reach a decrease in the flexural modulus of elasticity and the bending strength of below 10%. The stress-deformation

**TABLE 10** | Results of three-point bending tests.

| Composite sample | $E_f$ (GPa) | $\sigma_{fM}$ (MPa) | $\varepsilon_M$ (%) |
|---|---|---|---|
| TRAC REF composite | 22.68 ± 0.86 | 818.4 ± 25.2 | 4.03 ± 0.28 |
| TRAC 5%P APP 5% $TiO_2$ composite | 22.70 ± 0.63 | 786.9 ± 33.9 | 3.77 ± 0.11 |

*Note:* $E_f$, flexural modulus; $\sigma_{fM}$, bending strength; $\varepsilon_M$, deformation at the bending strength.

**TABLE 11** | Charpy impact strength of unnotched composite samples.

| Composite sample | Unnotched Charpy impact strength (kJ/m²) |
|---|---|
| TRAC REF composite | 304.6 ± 15.9 |
| TRAC 5%P APP 5% $TiO_2$ composite | 251.1 ± 18.8 |

curves from five parallel flexural tests for the reference and flame retarded samples are shown in Figure 8, while the corresponding average values are listed in Table 10.

The flexural modulus remained in the same region as the reference, while the addition of the flame retardant additive system and applying the porosity-reducing method detailed in chapter 3.7 resulted in only 3.8% reduction in the bending strength. The nearly unchanged flexural modulus indicates that the laminate's global stiffness is preserved despite the incorporation of solid flame-retardant additives. This confirms that fiber-dominated load transfer remains unaffected and that the optimized processing successfully prevented stiffness loss typically associated with increased porosity. The minor reduction in bending strength is primarily due to local stress concentrations introduced by particulate additives rather than to changes in fiber architecture or matrix integrity. The similarity of the stress-deformation curves further suggests that the composite's failure mechanism remained unchanged, indicating good compatibility between the epoxy matrix and the flame-retardant system. Overall, the results demonstrate that effective flame retardancy was achieved without compromising structural bending performance, fulfilling the initially defined mechanical design criteria.

### 3.9 | Charpy Impact Strength

The Charpy impact test is also based on three-point bending, but it applies a dynamic load to the sample. Similar to bending strength, we expected a slight decrease in impact strength. However, we also aimed to keep the reduction below 10%, relying on the optimized manufacturing process. According to the results (Table 11), the unnotched Charpy impact strength decreased by 17.6%, which does not meet the set target but is below 20%; thus, it can be considered acceptable.

Figure 9 shows the specimens after the Charpy impact tests. Both the reference and the flame retarded samples showed a catastrophic failure and significant delamination during the test. Therefore, the interlaminar strength should be improved in the future.

The larger reduction in impact resistance under dynamic loading compared to quasi-static bending highlights the greater sensitivity of impact resistance to local heterogeneities and interfaces introduced by solid additives. Impact loading promotes rapid crack initiation and propagation along interlaminar regions, explaining the pronounced delamination visible after testing. The similar macroscopic failure modes of the reference and flame-retarded composites indicate that the additive system does not fundamentally alter the fracture mechanism but slightly lowers energy absorption capability. The results suggest that future optimisation should focus on improving interlaminar toughness, for example, through interface modification or toughening strategies, while maintaining the achieved fire performance. Despite the moderate decrease, the impact performance remains within an acceptable engineering range for structural applications requiring enhanced fire safety.

### 3.10 | Electrical Resistivity

As the developed composite is intended for battery casing applications, its electrical resistivity is a critical parameter. Neat polymers are inherently electrically insulating; however, the incorporation of fibers and/or additives (especially salts) can increase the electrical conductivity and thereby reduce resistivity once the percolation threshold is reached. In this work, the aim was to maintain the electrical resistivity of the flame-retarded composites at a level comparable to that of the reference material. The measured electrical resistivity values of the samples are listed in Table 12.

The electrical resistivity decreased by only approximately 1.7%, remaining essentially at the same level as the reference sample, which is favorable for the intended application as battery casings. This minor change indicates that the 5%P APP 5% $TiO_2$ additive system does not introduce significant conductive pathways, preserving the insulating properties of the composite. The result also confirms that the combination of flame retardants and inert glass fibers does not compromise electrical safety, which is critical for preventing short circuits in battery enclosures. Maintaining high resistivity alongside improved flame retardancy highlights the balanced design of the composite, demonstrating that thermal and fire-performance enhancements can be achieved without adversely affecting electrical insulation. These findings suggest that the optimized formulation is suitable for electrically sensitive applications where both fire protection and insulation are required.

**TABLE 12** | Electrical resistivity of the TRAC reference and TRAC 5%P APP 5% $TiO_2$ composites.

| Composite sample | Electric resistivity (MΩ) |
|---|---|
| TRAC REF composite | 4.733 ± 0.071 |
| TRAC 5%P APP 5% $TiO_2$ composite | 4.652 ± 0.035 |

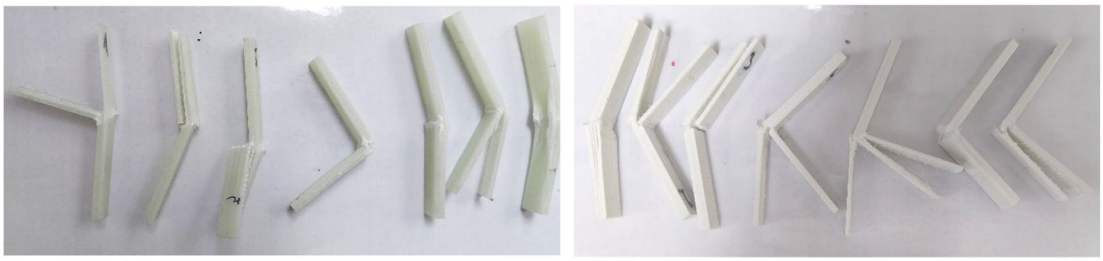


**FIGURE 9** | The composite samples after the Charpy impact test. (a) TRAC reference composites, (b) TRAC 5%P APP 5% $TiO_2$ composites.

### 3.11 | Filtering of the Solid Additives

Finally, we investigated the particle distribution of the flame retardant additives in the cross-section of the final composite system. When using solid additives in the resin matrix, the particles can be filtered out by the fiber reinforcement. This filtration phenomenon depends on the ratio of particle size to pore size in the fibrous media. Hand lamination and hot-pressing methods are less sensitive to filtration, but in injection-based techniques (e.g., vacuum infusion, resin transfer molding (RTM), vacuum-assisted RTM), filtration can be significant. This phenomenon results in an uneven particle distribution and, therefore, uneven properties across the cross-section of a composite part, which can be crucial for fire performance [23].

To determine the distribution of the phosphorus and titanium-containing flame retardants, samples were cut from the flame retarded composites and mapped by scanning electron microscopy coupled with energy dispersive spectrometry (SEM-EDS) at 30× magnification. The signals from the elements (phosphorus (P) and titanium (Ti)) were recorded, and the resulting P and Ti maps, along with the SEM image of the composite cross-section, were superimposed to determine the distribution of P and Ti across the entire cross-section. Based on the SEM-EDS elemental

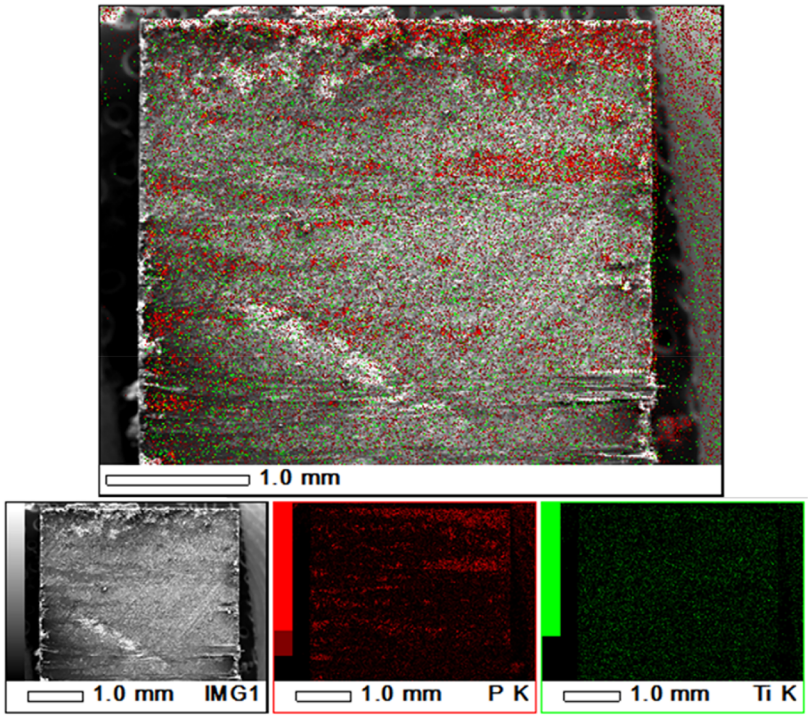


(a) distribution of P (red) and Ti (green) in the cross-section

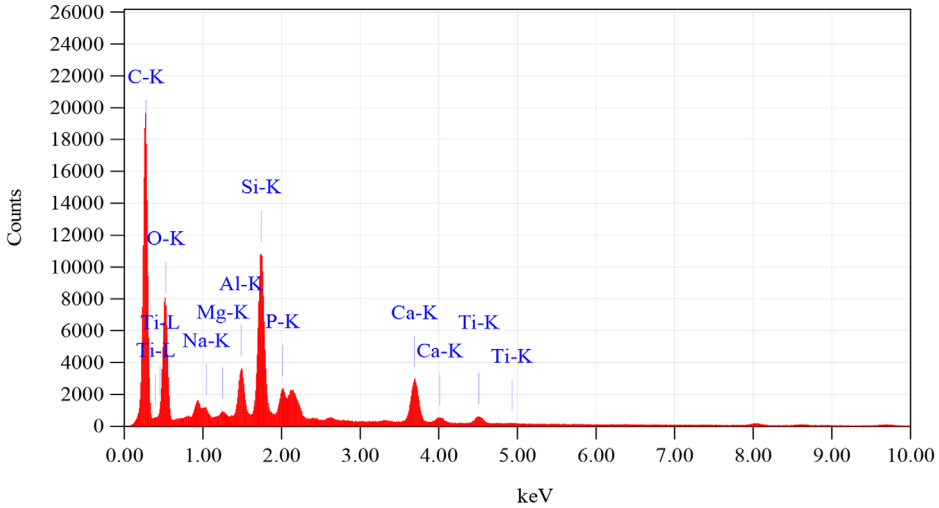


(b) elemental mapping of the cross-section

**FIGURE 10** | SEM-EDS results of TRAC 5%P APP 5% $TiO_2$ composite. (a) distribution of P (red) and Ti (green) in the cross-section, (b) elemental mapping of the cross-section.

maps (Figure 10), it can be concluded that for phosphorus, and consequently APP, there is a slight filtration in the direction of the injection, whereas the distribution of titanium, and thus titanium dioxide, is largely homogeneous. This indicates that $TiO_2$ is less prone to segregation during processing due to its much smaller particle size and better compatibility with the matrix-fiber system. The findings highlight the importance of matching the additive particle size to the fiber pore structure to ensure uniform distribution and consistent composite properties. For industrial applications, using APP with a particle size smaller than the reinforcement fibers' pore size would minimize filtration, improving additive homogeneity and overall performance. In this study, the APP used had an average particle size of 15 μm, but commercial APP with smaller particle sizes is available and may be more suitable for future manufacturing. Maintaining a uniform additive distribution is critical not only for fire performance but also for mechanical consistency, as local variations in particle concentration could affect stiffness, strength, and impact resistance. The SEM-EDS results confirm that, despite minor filtration of APP, the overall distribution is acceptable for the intended applications, but further optimisation may be beneficial for large-scale production.

## 4 | Conclusions

This work demonstrated that the fire performance of glass fiber-reinforced epoxy composites can be significantly enhanced through the synergistic combination of phosphorus-based and inorganic flame retardants, without substantial deterioration of thermomechanical or electrical properties.

The APP-$TiO_2$ system exhibited a clear synergistic effect, resulting in enhanced flame retardancy at both matrix and composite levels. The observed 53% reduction in peak heat release rate and the achievement of UL-94V-0 classification and 960/4.0 glow wire flammability index are attributed to stabilized condensed-phase protection, where APP-induced char formation is reinforced by $TiO_2$ through the development of a coherent ceramic–phosphate protective layer that effectively limits heat and mass transfer during combustion.

A key outcome of the study is that the use of solid flame retardants with suitable morphology allows the preservation of glass transition temperature and stiffness, thereby mitigating the commonly observed trade-off between fire performance and mechanical properties. The $T_g$ remained above 135°C for all formulations, and the reduction in flexural strength was limited to below 10%, indicating that structural performance can be retained with appropriate formulation and processing.

Processing conditions were found to play a critical role in determining composite quality. The optimization of the curing protocol, combined with moisture control and the use of anti-foaming agents, significantly reduced porosity, which in turn contributed to improved and more reproducible mechanical performance.

The study also highlighted the importance of particle-fiber interactions, demonstrating that filtration of solid additives depends strongly on the ratio of particle size to reinforcement pore size. While only minor filtration effects were observed under compression molding conditions, this aspect is expected to be critical for liquid molding technologies, and thus must be considered in material design for industrial applications.

Overall, the results indicate that multifunctional epoxy composites with balanced fire, mechanical, and electrical performance can be achieved through a combined approach involving formulation design, processing optimisation, and microstructural control. Future work should focus on improving interlaminar properties and impact resistance, as well as tailoring particle size distributions to ensure homogeneous additive dispersion in scalable manufacturing processes.

### Author Contributions

**Ákos Pomázi:** investigation, writing – original draft, validation, visualization. **Zsófia Kovács:** investigation, writing – review and editing, visualization, validation. **Beáta Szolnoki:** investigation, writing – review and editing, visualization, conceptualization. **Gábor Szebényi:** conceptualization, funding acquisition, writing – review and editing, project administration, supervision, resources, visualization, investigation. **Andrea Toldy:** conceptualization, funding acquisition, writing – original draft, writing – review and editing, project administration, resources, supervision, visualization.


### Acknowledgments

This research was funded by the National Research, Development and Innovation Office (NKFIH K142517, FK 142540, and STARTING 150473). The authors acknowledge the technical support of Bertalan Papp in preparation works and the help of Gergő Zsolt Marton in porosity tests, as well as the professional guidance provided by Thierry Renault (COMPOSITEC, France) in the development of the battery housing. This project has received funding from the European Union's Horizon 2020 research and innovation programme within the framework of the AMULET Project funded under grant agreement No 101005435. Beáta Szolnoki acknowledges the financial support received through the János Bolyai Scholarship from Hungarian Academy of Sciences. During the preparation of this work the authors used ChatGPT and Grammarly in order to improve the language and readability of the paper. After using these tools, the authors reviewed and edited the content as needed and take full responsibility for the content of the published article.

### Funding

This work was supported by National Research, Development and Innovation Office (grant nos. 142517, 142540, 150473), HORIZON EUROPE Framework Programme (grant no. 101005435), Magyar Tudományos Akadémia, János Bolyai Scholarship.


### Conflicts of Interest

The authors declare no conflicts of interest.

### Data Availability Statement

The data that support the findings of this study are available on request from the corresponding author. The data are not publicly available due to privacy or ethical restrictions.

### References


1. A. Toldy, "Safe and Sustainable-By-Design: Redefining Polymer Engineering for a Greener Future," *Express Polymer Letters* 19 (2025): 350, https://doi.org/10.3144/expresspolymlett.2025.25.

2. F. Khan, N. Hossain, J. J. Mim, et al., "Advances of Composite Materials in Automobile Applications—A Review," *Journal of Engineering Research* 13, no. 2 (2025): 1001–1023, https://doi.org/10.1016/j.jer.2024.02.017.

3. C. Koffler and K. Rohde-Brandenburger, "On the Calculation of Fuel Savings Through Lightweight Design in Automotive Life Cycle Assessments," *International Journal of Life Cycle Assessment* 15 (2010): 128–135, https://doi.org/10.1007/s11367-009-0127-z.

4. H. C. Kim, T. J. Wallington, J. L. Sullivan, and G. A. Keoleian, "Commentary on "Correction to: On the Calculation of Fuel Savings Through Lightweight Design in Automotive Life Cycle Assessments" by Koffler and Rohde-Brandeburger (2018)," *International Journal of Life Cycle Assessment* 24 (2019): 397–399, https://doi.org/10.1007/s11367-019-01584-z.

5. X.-H. Shi, X.-L. Li, Y.-M. Li, Z. Li, and D.-Y. Wang, "Flame-Retardant Strategy and Mechanism of Fiber Reinforced Polymeric Composite: A Review," *Composites Part B: Engineering* 233 (2022): 109663, https://doi.org/10.1016/j.compositesb.2022.109663.

6. A. Toldy, "Flame Retardancy of Carbon Fibre Reinforced Composites," *Express Polymer Letters* 12, no. 3 (2018): 186, https://doi.org/10.3144/expresspolymlett.2018.17.

7. B. Szolnoki, K. Bocz, P. L. Sóti, et al., "Development of Natural Fibre Reinforced Flame Retarded Epoxy Resin Composites," *Polymer Degradation and Stability* 119 (2015): 68–76, https://doi.org/10.1016/j.polymdegradstab.2015.04.028.

8. S. Liang, N. M. Neisius, and S. Gaan, "Recent Developments in Flame Retardant Polymeric Coatings," *Progress in Organic Coatings* 76, no. 11 (2013): 1642–1665, https://doi.org/10.1016/j.porgcoat.2013.07.014.

9. Á. Pomázi and A. Toldy, "Multifunctional Gelcoats for Fiber Reinforced Composites," *Coatings* 9, no. 3 (2019): 9030173, https://doi.org/10.3390/coatings9030173.

10. Á. Pomázi and A. Toldy, "Development of Fire Retardant Epoxy-Based Gelcoats for Carbon Fibre Reinforced Epoxy Resin Composites," *Progress in Organic Coatings* 151 (2021): 106015, https://doi.org/10.1016/j.porgcoat.2020.106015.

11. R. Ma and S. Wang, "Impact of APP Modified With DOPO Group-Containing Silane Coupling Agent on Flame Retardancy and Mechanical Properties of Epoxy Resin," *Journal of Applied Polymer Science* 142, no. 40 (2025): e57554, https://doi.org/10.1002/app.57554.

12. Z. Hu, Z. Wang, and S. Wang, "Effects of PAPP Modified by Silane Coupling Agent on the Mechanical and Flame-Retardant Properties of Epoxy Resin," *Journal of Macromolecular Science, Part A* 62, no. 9 (2025): 783–794, https://doi.org/10.1080/10601325.2025.2554327.

13. X. Wang and S. Wang, "Iron-Based MOF With Rodlike Morphology Boosting Flame Retardancy and Mechanical Strength of Epoxy Containing Ammonium Polyphosphate," *Journal of Materials Science* 61 (2026): 240–256, https://doi.org/10.1007/s10853-025-11774-w.

14. A. Toldy, B. Szolnoki, and G. Marosi, "Flame Retardancy of Fibre-Reinforced Epoxy Resin Composites for Aerospace Applications," *Polymer Degradation and Stability* 96 (2011): 371–376, https://doi.org/10.1016/j.polymdegradstab.2010.03.021.

15. A. Toldy, P. Niedermann, Z. Rapi, and B. Szolnoki, "Flame Retardancy of Glucofuranoside Based Bioepoxy and Composites Made Thereof," *Polymer Degradation and Stability* 142 (2017): 62–69, https://doi.org/10.1016/j.polymdegradstab.2017.05.024.

16. Á. Pomázi, B. Szolnoki, and A. Toldy, "Flame Retardancy of Low-Viscosity Epoxy Resins and Their Carbon Fibre Reinforced Composites via a Combined Solid and Gas Phase Mechanism," *Polymers* 10, no. 10 (2018): 1081, https://doi.org/10.3390/polym10101081.

17. W. Liu, D. Zhao, Z. Pan, Y. Shen, and T. Wang, "Enhanced Residue Stability and Strength of Epoxy-Based Coating for Fire Protection via Ceramifiable Strategy," *Progress in Organic Coatings* 154 (2021): 106211, https://doi.org/10.1016/j.porgcoat.2021.106211.

18. Y. Lei, X. Zhao, L. Xu, et al., "Natural Flame Retardant Minerals for Advanced Epoxy Composites," *Fire* 7, no. 9 (2024): 308, https://doi.org/10.3390/fire7090308.

19. M. Rajaei, D.-Y. Wang, and D. Bhattacharyya, "Combined Effects of Ammonium Polyphosphate and Talc on the Fire and Mechanical Properties of Epoxy/Glass Fabric Composites," *Composites Part B: Engineering* 113 (2017): 381–390, https://doi.org/10.1016/j.compositesb.2017.01.039.

20. X. Chen, Y. Wang, and C. Jiao, "Influence of $TiO_2$ Particles and APP on Combustion Behavior and Mechanical Properties of Flame-Retardant Thermoplastic Polyurethane," *Journal of Thermal Analysis and Calorimetry* 132 (2018): 251–261, https://doi.org/10.1007/s10973-017-6847-6.

21. H. Li, Z. Hu, S. Zhang, et al., "Effects of Titanium Dioxide on the Flammability and Char Formation of Water-Based Coatings Containing Intumescent Flame Retardants," *Progress in Organic Coatings* 78 (2015): 318–324, https://doi.org/10.1016/j.porgcoat.2014.08.003.

22. Z. Wang, E. Han, and W. Ke, "Effect of Nanoparticles on the Improvement in Fire-Resistant and Anti-Ageing Properties of Flame-Retardant Coating," *Surface and Coatings Technology* 200, no. 20–21 (2006): 5706–5716, https://doi.org/10.1016/j.surfcoat.2005.08.102.

23. A. Toldy, Á. Pomázi, and B. Szolnoki, "The Effect of Manufacturing Technologies on the Flame Retardancy of Carbon Fibre Reinforced Epoxy Resin Composites," *Polymer Degradation and Stability* 174 (2020): 109094, https://doi.org/10.1016/j.polymdegradstab.2020.109094.